Rate-Independent Self-Healing Double Network Hydrogels Using Thixotropic Sacrificial Network

*Tomoki Yasui[1,2], Yong Zheng[3], Tasuku Nakajima[1,3], Eiji Kamio[2], Hideto Matsuyama[2], and Jian Ping Gong[1,3]**

1: Faculty of Advanced Life Science, Hokkaido University, N21W11, Kita-ku, Sapporo, Hokkaido 001-0021, Japan

2: Department of Chemical Science and Engineering, Research Center for Membrane and Film Technology, Kobe University, 1-1 Rokkodai-cho, Nada-ku, Kobe, Hyogo 657-8501, Japan

3: Institute for Chemical Reaction Design and Discovery (WPI-ICReDD), Hokkaido University, N21W10, Kita-ku, Sapporo, Hokkaido 001-0021, Japan

Table of Contents (TOC) graphic, for Table of Contents use only

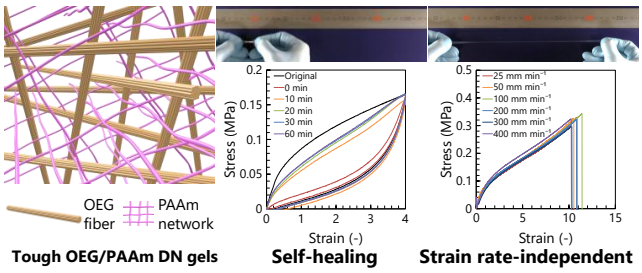

ABSTRACT

Tough and self-healing hydrogels can be developed by incorporating non-covalent dynamic bonds in the polymer network as reversible sacrificial bonds to dissipate energy. However, the dynamic nature of the non-covalent bonds results in strong strain rate dependency of the materials. In most applications, strain-rate independent mechanical performances are required. Developing tough self-healing hydrogels showing strain rate-independency is a challenge. In this study, we realize this by adopting thixotropic hydrogel of an oligomeric electrolyte gelator as brittle, though self-healing, sacrificial network of tough double network (DN) hydrogels. The hydrogels, synthesized via a facile one-pot approach, show specific features of typical double network materials, including high mechanical strength, strain softening, large mechanical hysteresis, but also self-healing and strain rate-independency. As the strain rate-independent and self-healing mechanical behavior of these novel hydrogels overcome the shortcomings of the existing DN hydrogels, these results expand the application spectrum of DN hydrogels.

INTRODUCTION

Hydrogels, which are three-dimensional networks swollen with a large amount of water, are promising soft materials for various applications, such as scaffolds for tissue engineering,[1, 2] drug delivery systems,[3-5] sensors,[6] and wound dressings.[7] However, utilization of hydrogels has been limited by their low mechanical strength.[8] In the past decades, several molecular strategies to strengthen the hydrogel have been developed to overcome the severe shortcomings of these materials.[8-12]

The double network (DN) concept is an effective approach for developing tough soft materials.[11, 13-18] A hydrogel with a DN structure, composed of interpenetrating rigid/brittle and soft/stretchable networks, exhibits significantly higher mechanical strength and toughness than the sum of its constituent networks. The rigid/brittle network acts as a fragile component that is easily fractured on deformation to dissipate the energy, whereas the soft/stretchable network maintains its integrity and provides high toughness to the material. Moreover, high toughness prevents crack propagation from initial defects in the material, thereby enhancing the mechanical strength of the DN hydrogel. The rigid/brittle network primarily serves as a sacrificial network and imparts high strength and toughness to these materials.

Two types of sacrificial networks (or bonds) exist. The first type is a covalently crosslinked rigid/brittle polymer network.[11, 13-18] As the bond energy of the covalent crosslinking is high, this type of sacrificial network dissipates a large amount of energy at deformation through covalent bond scission. This increases the toughness of the hydrogels dramatically. This type of DN hydrogels show strain rate-independent stress–strain curves owing to the elasticity of the covalently crosslinked sacrificial network.[13] However, the fracture of a covalent bond is usually irreversible. Therefore, once the covalent sacrificial network is fractured, it cannot recover its original structure, resulting in permanent softening although the stretchable network maintains the shape of the material.[14, 15, 17, 18] The second type of sacrificial network is based on a polymer network with numerous non-covalent intermolecular interactions, such as van der Waals interaction, hydrogen bonding, electrostatic interaction, and coordination bonds.[19-35] As these non-covalent interactions are dynamic and reversible, the fractured sacrificial network can heal after certain period of time. However, the dynamic nature of the non-covalent bonds in the sacrificial networks brings a strong strain rate-dependency in the stress–strain curves of the materials.[24, 25, 30]

Thus, DN hydrogels composed of covalent sacrificial networks exhibit strain rate-independency but permanent strain softening, whereas those composed of non-covalent sacrificial networks are self-healable but exhibit strain rate-dependency. The aim of this study is to develop tough DN hydrogels displaying strain rate-independent deformation and reasonably fast self-healing.

Thixotropic gels are gels which exhibit thixotropy. A thixotropic gel (solid) becomes a sol (liquid) under shear stress and recovers its gel state when the stress is removed. Thixotropic behavior of a material is primarily a structural effect and is accompanied by the spontaneous dissipation of excess internal energy. Hence, we expect that thixotropic gels could be used as reversible sacrificial networks in DN hydrogels. More importantly, thixotropic materials usually show elastic-like deformation before structure rupture, and therefore, DN hydrogels prepared from thixotropic gels as sacrificial networks are likely to show both strain rate-independent deformation and self-healing of sacrificial network. In this study, we adopted thixotropic hydrogels composed of an oligomeric electrolyte gelator (OEG) based on poly(pyridinium-1,4-diyliminocarbonyl-1,4-phenylenemethylene chloride) (Scheme 1). The physical OEG gels, with a quasi-solid state (loss factor $\tan \delta \approx 0.1$), show unique rheological behavior and an almost frequency independent storage modulus (G') over a wide dynamic frequency window (0.05–100 rad/s), similar to that of the chemical hydrogels.[36-41] Above a very small critical strain ($\varepsilon_c > 0.1$), G' of OEG gels dramatically decreases, showing a quasi-liquid state ($\tan \delta > 1$), and immediately recovers, indicating the solid state upon stress removal.[36, 39, 40] The rheological behavior of thixotropic OEG gels suggests their potential as a brittle, strain rate-independent, and self-healable sacrificial network in DN hydrogels.

Herein, DN hydrogels were prepared using OEG gel as the sacrificial network and a polyacrylamide (PAAm) network as the soft and stretchable matrix. Such DN hydrogels could be synthesized by a facile one-pot sequential process, owing to different formation mechanisms of

the two networks. The OEG network is formed by the self-assembly of OEG molecules, whereas the PAAm network is formed by free radical polymerization of AAm monomers and crosslinkers. The one-pot synthesis permits us to prepare the DN hydrogels in various complex shapes. The OEG/PAAm DN hydrogels exhibit not only the self-healing property of the OEG network but also a negligible strain rate-dependency in the stress–strain curves. This study provides a facile strategy to overcome the shortcomings of the existing DN hydrogels based on conventional non-covalent and covalent sacrificial networks, and significantly expands the application spectrum of hydrogels.

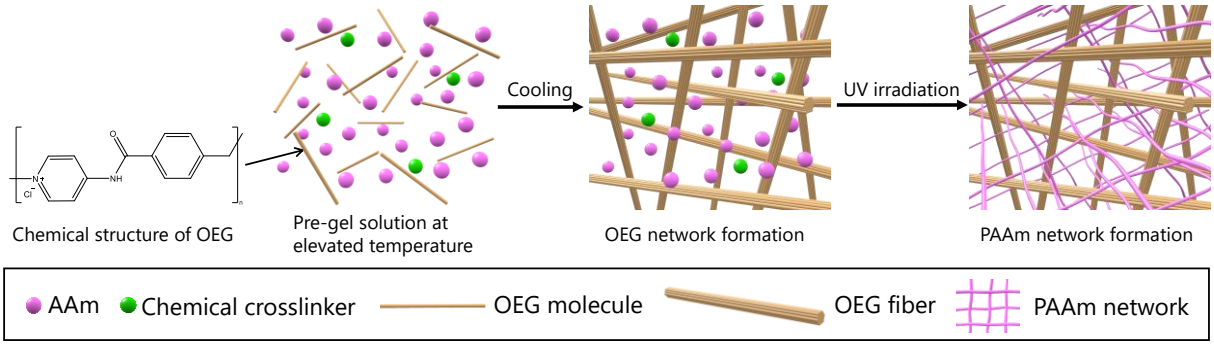

Scheme 1. Schematic of one-pot sequential synthesis of OEG/PAAm double network hydrogels.

EXPERIMENTAL SECTION

Materials

4-Aminopyridine and 4-(chloromethyl)benzoyl chloride were purchased from Tokyo Chemical Industry. Triethylamine, *N*,*N'*-methylenebis(acrylamide) (MBAA), 2-oxoglutaric acid (OA), sodium chloride (NaCl), dichloromethane, and ethanol were purchased from FUJIFILM Wako Pure Chemicals Corporation. Acrylamide (AAm) was purchased from Junsei Chemical Co. Ltd.

DCM was dried using molecular sieves (3 Å, FUJIFILM Wako Pure Chemicals Corporation) prior to usage. All reagents and chemicals were used as received without further purification.

Synthesis of OEG

The OEG, poly(pyridinium-1,4-diyliminocarbonyl-1,4-phenylenemethylene chloride), was synthesized via a method reported previously.[36] The reaction scheme is shown in Scheme S1. A solution of 4-(chloromethyl)benzoyl chloride (53 mmol) in dichloromethane (40 ml) was added to a suspension of 4-aminopyridine (53 mmol) and triethylamine (58 mmol) in dichloromethane (80 ml). The mixture was then heated under reflux for 24 h. After cooling, the precipitates were filtered, washed with dichloromethane and ethanol, followed by vacuum drying at 50 °C for 3 h. The structure of OEG was confirmed using ^{1}H-NMR spectroscopy (Unity INOVA 500, Agilent Technologies, USA). ^{1}H NMR (500 MHz, D_2O, δ): 8.76 (2H), 8.29 (2H), 8.03 (2H), 7.62 (2H), 5.8 (2H) were observed, which were consistent with the previous report.[36] In the literature, the synthesized OEG has n = 22.[38]

Preparation of OEG/PAAm DN hydrogels

The OEG/PAAm DN hydrogels were prepared via one-pot sequential formation of OEG and PAAm networks. Typically, OEG powder (0.4 g) was added to Milli-Q water (6.0 g). After ultrasonication to disperse the OEG powder, AAm (1.6 g), MBAA (3.5 mg, 0.1% of AAm in moles), and OA (3.3 mg, 0.1% of AAm in moles) were added to the suspension. The suspension was heated and stirred on a hot plate until complete dissolution of the OEG powder. The obtained clear solution was then poured into a glass mold, consisting of two glass plates and a 1 mm thick silicone rubber spacer. To avoid rapid cooling of the solution, the glass mold was heated to 100 °C

before pouring the solution. The OEG network was formed by cooling the solution to approximately 25 °C. Then, photo-initiated free radical polymerization was performed in an argon filled chamber under ultraviolet (UV) light (365 nm, 4 mW cm^{-2}) for 8 h. The OEG and PAAm concentrations in this gel were 5 wt.% and 20 wt.%, respectively. The PAAm content was controlled to 20 wt.% in all the OEG/PAAm DN hydrogels.

For comparison, the PAAm SN gels were prepared without OEG. Typically, AAm (1.6 g), MBAA (3.5 mg, 0.1% of AAm in moles), and OA (3.3 mg, 0.1% of AAm in moles) were added to 6.4 g of Milli-Q water (6.4 g). The mixture was stirred until complete dissolution and then poured into a similar glass mold, as described earlier. The conditions of photo-initiated free radical polymerization were the same as those described earlier. The PAAm content in the PAAm SN hydrogels was 20 wt.%.

Polarized microscopy

The OEG network in the OEG/PAAm DN hydrogel sheet (thickness = 1 mm) was observed using polarized microscopy (BH-2, Olympus Corporation, Japan).

Rheological measurement

The rheological properties of the OEG gel with AAm monomer and OEG/PAAm DN hydrogel were measured using a rheometer (ARES G2, TA Instruments, USA). A parallel plate with 25 mm diameter was used for the rheological measurements. During the rheological test, the temperature was maintained at 25 °C.

Differential scanning calorimetry (DSC) analysis

The DSC (Discovery DSC2500, TA Instruments, USA) analysis of the hydrogels was performed to evaluate the gel–sol transition of the OEG gel network. A small piece of the hydrogel, hermetically sealed in an aluminum pan, was heated from 25 °C to 100 °C at a rate of 10 °C min^{-1}.

Tensile tests

Uniaxial tensile testing of as-prepared OEG/PAAm DN hydrogels was performed using a universal testing machine (Instron 5965, Instron Co., USA) at 25 °C. Dumbbell-shaped specimens, as per JIS K6251-7 standard (gauge length = 12.0 mm, width = 2.0 mm, thickness = 1.0 mm) were stretched at a constant extension rate of 100 mm min^{-1}. To evaluate the strain rate-dependency, the extension rate was varied from 25 mm min^{-1} to 400 mm min^{-1}. In the cyclic loading–unloading tests, the stretching and return operations were performed at an extension rate of 100 mm min^{-1} till a maximum strain of 8.0 with a step size of 2.0.

Self-recovery tests

Dumbbell-shaped specimens as per JIS K6251-7 standard (gauge length = 12.0 mm, width = 2.0 mm, thickness = 1.0 mm) were stretched at an extension rate of 100 mm min^{-1} until a strain of 4.0 was realized and then immediately returned to the initial position at the same rate (first cycle). The samples were then detached from the apparatus and annealed at certain temperature (25 °C and 50 °C) for predetermined times. To prevent water evaporation from the hydrogels, the specimens were tightly wrapped in individual polyethylene bags during annealing. After annealing, cyclic loading–unloading test was performed again (second cycle). From the cyclic loading–unloading

curves, the dissipated energy (U) and Young's modulus (E) were determined. The dissipated energy was calculated from the area between the loading and unloading curves using the following equation:

$$U = \int_0^4 \sigma \, \mathrm{d}\varepsilon \Big|_{\text{loading}} - \int_0^4 \sigma \, \mathrm{d}\varepsilon \Big|_{\text{unloading}} \quad (1)$$

where σ and ε are stress and strain, respectively. The extent of recovery was determined using the dissipated energies and Young's moduli of the samples before and after annealing. The recovery ratios of the Young's modulus and dissipation energy were defined as E_2/E_1 and U_2/U_1, respectively, where the subscripts "1" and "2" indicate the values after first and second cyclic loading, respectively.

RESULTS AND DISCUSSION

Preparation of OEG/PAAm DN Hydrogels

The OEG/PAAm DN hydrogels were prepared via sequential network formation of the OEG and PAAm networks in a one-pot synthesis, enabling the obtainment of hydrogels in various shapes, such as films, rods, cylinder, and flower, using appropriate molds (Figure 1a–d). These OEG/PAAm DN hydrogels could be stretched significantly without fracture, in similar to conventional DN gels made from covalent or non-covalent sacrificial networks (Figure 1e and f). The formation of the OEG network was confirmed by gelation before PAAm formation (Figure S1), gel turbidity (Figure 1), and birefringence under crossed nicols configuration[37] (Figure S2). The results of the aforementioned analysis confirmed the successful preparation of OEG/PAAm DN hydrogels, with excellent stretchability, in various shapes.

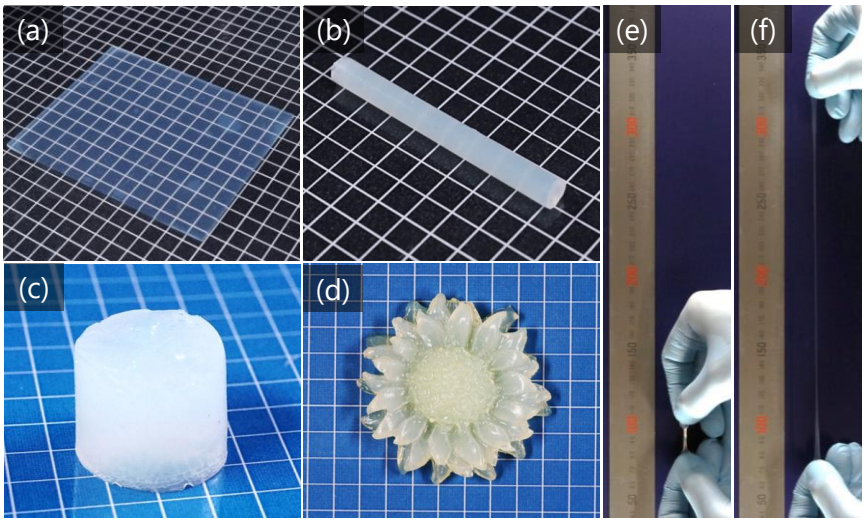

Figure 1. Digital photographs of OEG/PAAm DN hydrogels in various shapes, such as (a) film, (b) rod, (c) cylinder, and (d) flower. The OEG/PAAm DN hydrogels before (e) and under (f) stretching. The grid size in (a)–(d) is 5 mm. The OEG content, PAAm content, and MBAA concentration in gels are 5 wt.%, 20 wt.%, and 0.1% of AAm in moles, respectively.

Rheological property of OEG gel with AAm monomer and OEG/PAAm DN hydrogel

To confirm the OEG network-based rheological properties in PAAm network, we evaluated thixotropic property of the OEG gel with AAm monomer. As shown in Figure 2a, G' of the OEG gel with AAm monomer monotonically decreased with increase of strain. This trend is consistent with the OEG gel without AAm monomer.[36] When the applied strain was higher than 70%, the loss modulus G'' becomes higher than the storage modulus G', indicating that the gel becomes sol state. To study the self-recovery, we alternated the strain between 0.2% and 150% every 600 seconds. The result shown in Figure 2b demonstrate that the OEG gel with AAm monomer showed fast reversible gel–sol transition in response to the change in strain. As shown in Figure 2c, d and Video S1, the OEG gel with AAm monomer becomes sol state after vortex mixing, confirming the

thixotropic property. The frequency dependence of G' of the OEG gel with AAm monomer and OEG/PAAm DN gel are shown in Figure 2e and f. The G' of OEG gel with AAm monomer was almost constant over a wide dynamic frequency window (0.1–100 rad/s), further confirming its thixotropic property. The OEG/PAAm DN gel exhibited very similar dynamic behavior of G' with that of the OEG gel. These results indicate that at small deformation, the OEG network dominates the rheological properties in the OEG/PAAm DN gels.

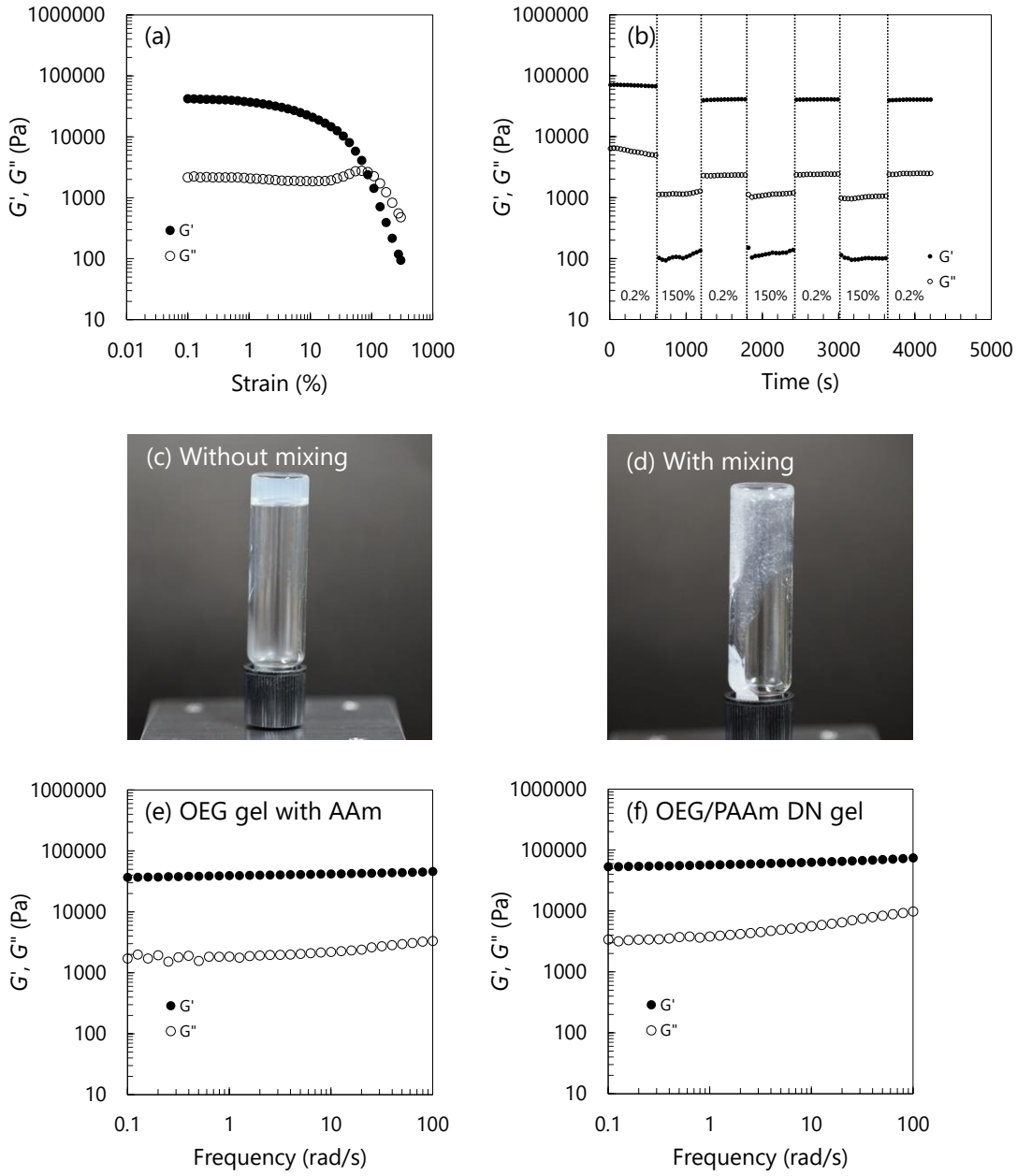

Figure 2. Rheological properties of OEG gel with AAm monomer and OEG/PAAm DN gel. (a) Strain dependence of G' and G'' of OEG gel with AAm. (b) Self-recovery behavior of OEG gel with AAm. The strain alternated between 0.2% and 150% every 600 seconds. (c, d) Digital photographs without (c) and with (d) vortex mixing of OEG gel with AAm. (e, f) Frequency dependence of G' and G'' of OEG gel with AAm (e) and OEG/PAAm DN gel (f). The frequency

used for (a) and (b) is 6.0 rad/s. The strain used for (e) and (f) is 0.2%. The OEG content and MBAA concentration in gels are 5 wt.% and 0.1% of AAm in moles, respectively.

Double network effect of OEG/PAAm DN hydrogels

Figure 3a shows the stress–strain curves of OEG/PAAm DN hydrogels with different OEG content and corresponding PAAm single network (SN) hydrogel. The tensile test of OEG gels could not be performed, as they fractured easily due to brittleness when removed from the molds. The OEG/PAAm DN hydrogels exhibited a higher fracture stress than that of the PAAm SN hydrogel, suggesting the role of OEG network in imparting high mechanical strength to the material. The effects of OEG content on the mechanical properties are shown in Figure 3b–d. The fracture stress of the hydrogels increased significantly with increasing OEG content (Figure 3b). By contrast, the fracture strain remained almost constant (Figure 3c). It can be stated that the fracture strain of the OEG/PAAm DN hydrogels is governed by the PAAm network, because of low fracture strain (0.1)[36] of OEG gels. As the PAAm networks were prepared with the same crosslinker and initiator concentrations, it was assumed that almost identical PAAm networks were formed in these OEG/PAAm DN hydrogels, which explains their nearly similar fracture strain values. The Young's modulus remained almost constant (0.03 MPa) up to 3 wt.% OEG content, after which it increased sharply with increasing OEG content. The Young's modulus of the OEG/PAAm DN hydrogel can be determined by the sum of that of OEG and PAAm networks. When the OEG content was 1 wt.%, the storage modulus of the OEG network was approximately 0.1 kPa,[36] which is much lower than that of the PAAm network. Therefore, the Young's modulus of the DN hydrogel with 1 wt.% OEG was almost the same as that of the PAAm SN hydrogel. These results clearly demonstrate that the OEG network enhanced the mechanical strength of the

hydrogels. The high fracture stress of the OEG/PAAm DN hydrogels also indicates that the fracture of the OEG network inside the hydrogels occur, because the stress concentration at the crack in the OEG network is suppressed by the PAAm network, like that in typical DN hydrogels.[14]

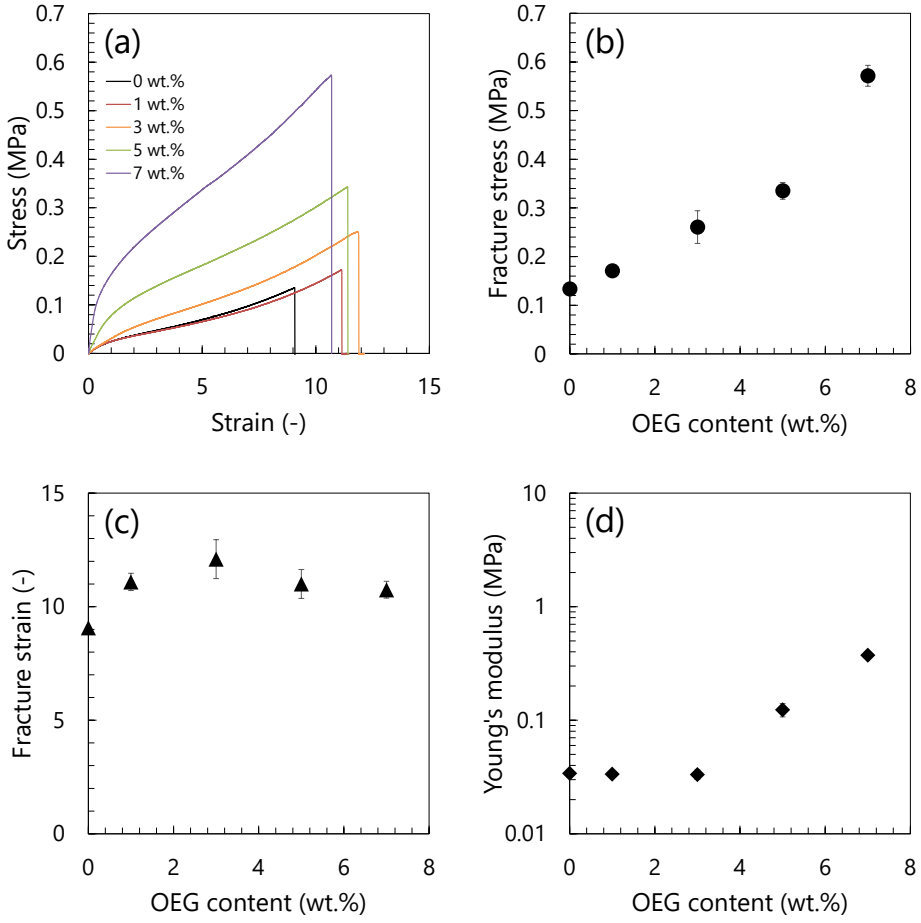

Figure 3. Mechanical properties of OEG/PAAm DN hydrogels with various OEG contents. (a) Stress–strain curves of OEG/PAAm DN hydrogels with various OEG contents. OEG content dependency of (b) fracture stress, (c) fracture strain, and (d) Young's modulus. The MBAA concentration in these gels is 0.1% of AAm in moles.

Cyclic loading–unloading tests (Figure 4) were performed to confirm the sacrificial nature of OEG network and the energy dissipation behavior. Ideally, the cyclic loading–unloading curves should exhibit large hysteresis if the OEG network acts as a sacrificial network and dissipates energy. As expected, the cyclic loading–unloading curves clearly showed hysteresis when the OEG content was above 3 wt.%. The loading curves almost overlapped with the unloading curves of the previous cycles before surpassing the strain of the previous cycle. Furthermore, the residual strain was very small. These characteristics are very similar to those of DN hydrogels composed of covalent networks.[18, 42] We notice that the stress of cyclic loading–unloading curves at large strain is slightly larger than that of non-cyclic curves in Figure 4b–d, due to slight drying of the hydrogel. The dissipated energy, represented by the enclosed area of a cyclic loading–unloading curve, linearly increased with the maximum strain applied to the gels. The dissipated energy also increased with increasing OEG content (≥ 3 wt.%) when compared at the same strain as shown in Figure 4e. By contrast, the PAAm SN hydrogel (Figure S3) and OEG/PAAm DN hydrogel with 1 wt.% OEG (Figure 4a) did not exhibit hysteresis. The hysteresis observed in the cyclic loading–unloading tests clearly demonstrates that the OEG network dissipated the energy via fracture. Intrinsically, the OEG network is composed of supramolecular fibers formed due to inter-OEG molecule interactions, including van der Waals forces, hydrogen bonding, electrostatic interactions, cation–π interactions, and π–π interactions.[36, 38] Therefore, the hysteresis observed in the cyclic loading–unloading curves could be attributed to the breaking of intermolecular interactions between the OEG molecules under stress. Thus, it can be concluded that the OEG/PAAm DN hydrogels showed higher mechanical strength owing to the sacrificial bond effect of the OEG network. The efficient fracture of the OEG network in the stretched OEG/PAAm DN hydrogels

could be attributed to the entanglements and/or hydrogen bonding between OEG and PAAm chains, which effectively enabled the stress transfer between OEG and PAAm networks.

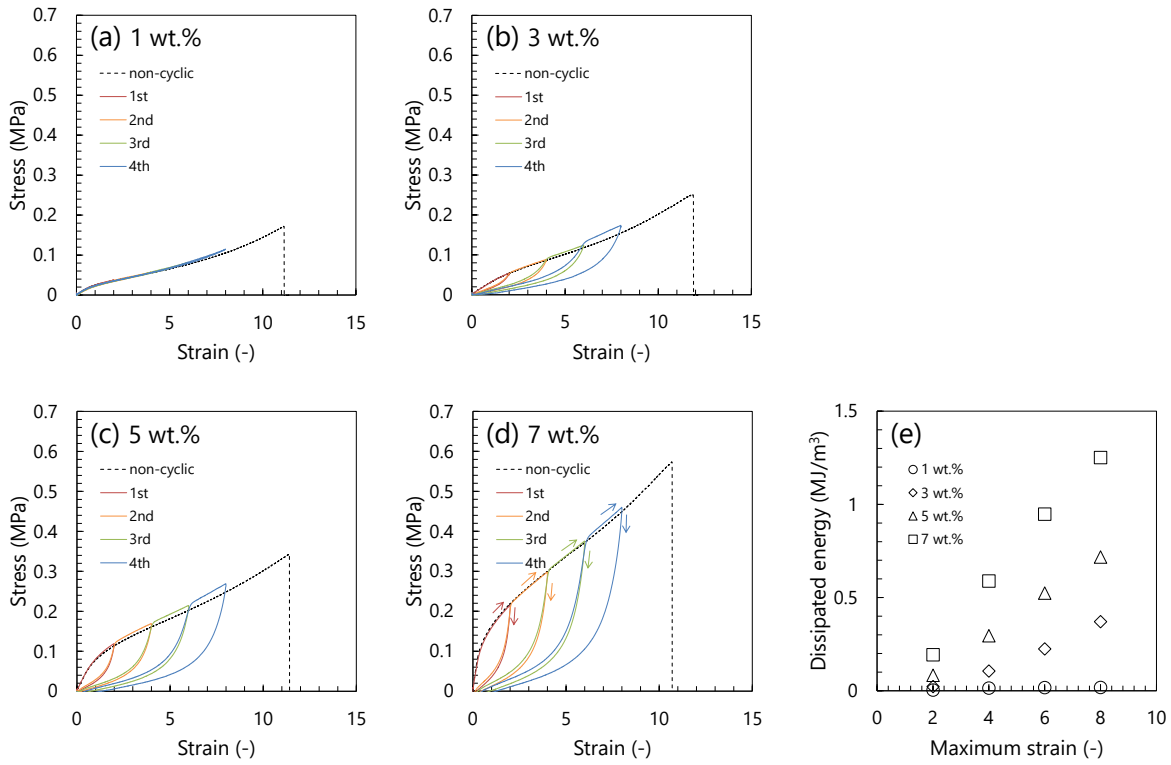

Figure 4. Cyclic loading–unloading curves of OEG/PAAm DN hydrogels with (a) 1 wt.%, (b) 3 wt.%, (c) 5 wt.%, and (d) 7 wt.% OEG content. For comparison, the non-cyclic stress–strain curves of Figure 3a are also shown as dotted lines in (a)–(d). The arrows in (d) show the deformation direction in each cycle as an example for all the cyclic curves. (e) Relationship between dissipated energy and maximum strain for the cyclic loading–unloading test. The MBAA concentration in these gels is 0.1% of AAm in moles.

Strain rate-independent deformation of OEG/PAAm DN hydrogels

Based on the unique mechanical behavior of the OEG network, i.e., the dynamic moduli plateau over a wide frequency range and self-healing properties,[36, 39, 40] the OEG/PAAm DN hydrogels are expected to show strain rate-independent but self-healable deformation.

The strain rate-independent deformation of the OEG/PAAm DN hydrogels was evaluated by tensile testing at various strain rates. In general, tough hydrogels with non-covalent sacrificial bonds exhibit a strong strain rate-dependency in the stress–strain curves.[24, 25, 30] This is attributed to the dynamic nature of the non-covalent bonds, marked by the characteristic bond lifetime. The modulus and fracture stress of the conventional tough hydrogels with non-covalent sacrificial bonds increase, whereas the fracture strain decreases with increasing strain rate.[24, 25, 30] In the present case, as shown in Figure 5, the stress–strain curves of the OEG/PAAm DN hydrogels (5 wt.% OEG) changed negligibly over a wide extension rate range of 25–400 mm min^{-1}, corresponding to an engineering strain rate range of 0.03–0.56 s^{-1}. These results indicate that the OEG network behaved as a brittle quasi-permanent network in the range of the strain rate applied in this study.

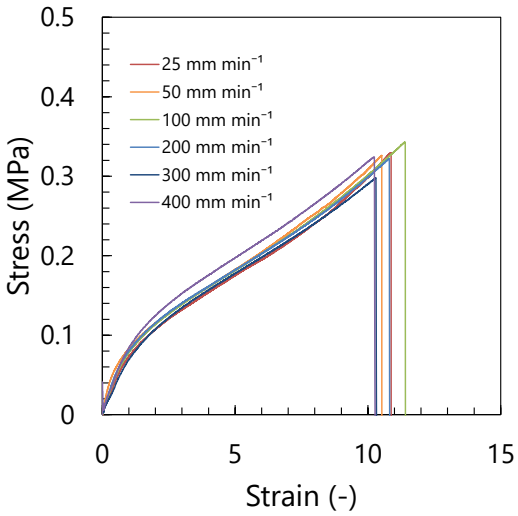

Figure 5. Stress–strain curves of OEG/PAAm DN hydrogels obtained at different extension rates. The OEG content and MBAA concentration in gels are 5 wt.% and 0.1% of AAm in moles, respectively.

Self-healing of sacrificial network in OEG/PAAm DN hydrogels

The self-healing properties of sacrificial network in the OEG/PAAm DN hydrogels were evaluated by the recovery of the cyclic loading–unloading curve. Figure 6a and b show the second loading–unloading curves of hydrogel specimens at 25 °C and 50 °C, respectively, with different waiting times after the first loading. The first loading–unloading curves are depicted as "original" curves in the figures. Partial recovery was observed, and the recovery efficiency at 50 °C was higher than that at 25 °C. As shown in Figure 6c and d, even at room temperature (25 °C), up to 40% of the Young's modulus and dissipated energy were recovered within 10 min. After 30 min of annealing at 50 °C, the recovery reached 90%. These results indicate that the fractured OEG network reformed due to the non-covalent nature of the OEG network. Such fast self-healing at relatively low healing temperature will greatly favors the practical use of tough DN gels.

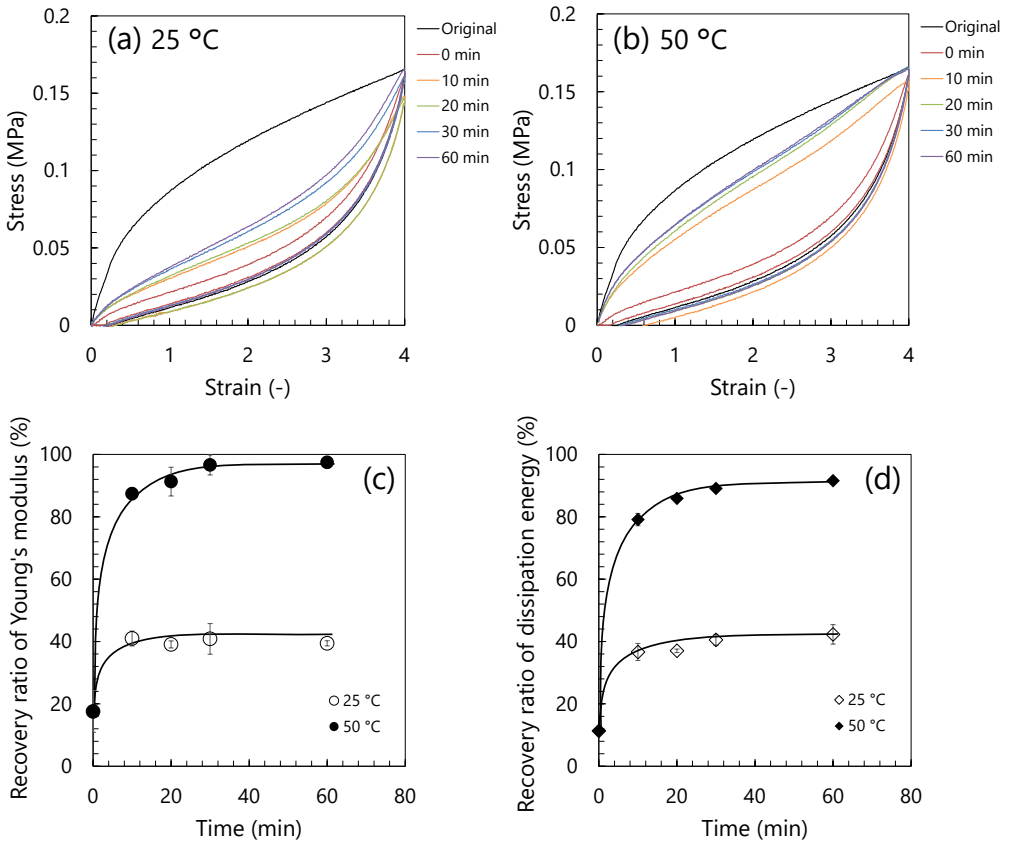

Figure 6. Self-healing properties of sacrificial network in OEG/PAAm DN hydrogel. (a, b) Second cyclic loading–unloading curves of specimens annealed at 25 °C (a) and 50 °C (b) for different times after first cycle. The curves marked "original" are first cyclic loading–unloading curves. (c, d) Waiting time dependence of recovery ratios of Young's modulus (c) and dissipation energy (d) of OEG/PAAm DN hydrogels. The OEG content and MBAA concentration in gels are 5 wt.% and 0.1% of AAm in moles, respectively. Measurements are performed at 25 °C.

These results further confirm the strain rate independency and self-recovery behavior of the OEG/PAAm DN hydrogels. The reason for this unique mechanical behavior can be attributed to the quasi-permanent network structure of OEG as revealed by the frequency-independent behavior of the dynamic modulus in the observed strain rate window, resulting in strain rate-independent

stress–strain curves. As previously stated, fibrous network structure is formed in OEG gels through various non-covalent interactions between OEG molecules.[36, 38] Although each individual non-covalent bond is weak, the probability of simultaneous breaking of all the bonds leading to fiber separation is very low due to the inherent rigidity of OEG oligomeric chains, which leads to cooperative bonding over the length scale of the persistence length of the OEG chains. Under a large stress, the fiber network fractures due to the breaking of non-covalent bonds, however, it does not flow as it is interpenetrated with the highly stretchable PAAm network. The rubber elasticity of the PAAm network ensures the reversion of fragmented fiber segments to their original position after stress removal, which then reforms the original brittle network under thermal annealing.

Interestingly, the self-healing of OEG network occurred even at temperatures lower than the gel–sol transition temperature of the OEG gels. The gel–sol transition of the OEG network does not occur below 50 °C as confirmed by the absence of an endothermic peak below 50 °C in the differential scanning calorimetry (DSC) curve of the OEG/PAAm DN hydrogel (Figure S4). The detailed analysis of thermal dependence of the OEG structure in OEG/PAAm DN hydrogels is beyond the scope of this work and will be reported in a future work.

Controlling the mechanical properties of OEG/PAAm DN hydrogels

The toughness of the OEG/PAAm DN hydrogels should be determined by the total extent of fracture of the OEG network at the failure, because the toughening mechanism of the OEG/PAAm DN hydrogels involves energy dissipation via fracture of the OEG network. Therefore, it was expected that the toughness of OEG/PAAm DN hydrogels could be controlled by the fracture strain of the hydrogels and the strength of inter-OEG molecule interactions.

The effect of chemical crosslinker concentration in the PAAm network on the mechanical strength of the OEG/PAAm DN hydrogels was evaluated because the fracture strain of the OEG/PAAm DN hydrogels was governed by the crosslink density of the PAAm network. As shown in Figure 7a–c, the fracture strains of the OEG/PAAm DN (5 wt.% OEG) and PAAm SN hydrogels are almost same and increase with decreasing MBAA concentration, suggesting the tunability of the fracture strain of OEG/PAAm DN hydrogels via MBAA concentration. This demonstrates that the fracture strain of OEG/PAAm hydrogels are determined by PAAm network because the fracture strain of the PAAm network (approximately 9–18) is much higher than that of OEG network (0.7, Figure 2a). Notably, the fracture strain value of the OEG/PAAm DN hydrogel decreased drastically when the MBAA concentration was lower than 0.02% relative to the AAm concentration in moles. This indicates that the PAAm network was too weak to sustain a large stress when the MBAA concentration was lower than 0.02%. This crosslinking threshold effect of the stretchable network was also observed in conventional chemically crosslinked DN gels.[43] Figure 7d shows the effect of MBAA concentration on the toughness, which is represented by the area under the stress–strain curve of the OEG/PAAm DN and PAAm SN hydrogels. The toughness of the OEG/PAAm DN hydrogels increased with decreasing MBAA concentration. This was attributed to the increased total dissipated energy caused by the increase in the extent of fracture of the OEG network with increasing fracture strain. These results clearly demonstrate the tunability of mechanical properties of the OEG/PAAm DN hydrogels via chemical crosslinker concentration.

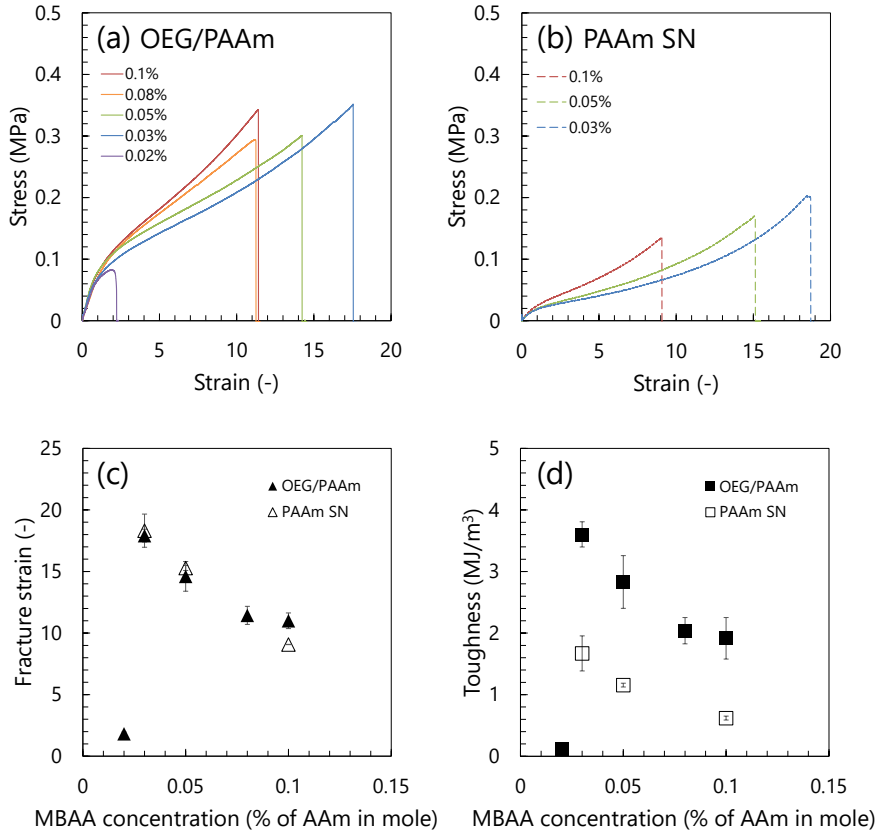

Figure 7. Effect of crosslinker (MBAA) concentration in PAAm network on the mechanical properties of OEG/PAAm DN hydrogels. Stress–strain curves of (a) OEG/PAAm DN and (b) PAAm SN hydrogels with different MBAA concentrations. MBAA concentration dependency of (c) fracture strain and (d) toughness of OEG/PAAm DN hydrogels. The OEG content of the OEG/PAAm DN hydrogels is 5 wt.%.

The effect of salt concentration on the mechanical strength of the OEG/PAAm DN hydrogels was also evaluated. The storage modulus of the OEG gels has been reported to increase with the addition of a small amount of salt because of strengthened inter-OEG molecule interactions.[40] Therefore, the mechanical strength of the OEG/PAAm DN hydrogels was expected to increase with increasing salt concentration. Figure 8 shows the effect of NaCl concentration on the

mechanical behavior of the OEG/PAAm DN hydrogels. As shown in Figure 8a, b, and d, the fracture stress and Young's modulus of the OEG/PAAm DN hydrogels increased with increasing salt concentration till 150 mM. Beyond this salt concentration, the fracture stress and Young's modulus decreased. This tendency is consistent with a previous report on OEG gels and was explained by equilibrium shifts of the complexation state of the OEG molecules.[40] It was suggested that increasing the NaCl concentration suppresses the electrostatic repulsion between the OEG molecules and increases their complexation. At high concentrations (> 150 mM), the OEG molecules become heavily aggregated, leading to the collapse of OEG network due to precipitation. The aggregation of OEG molecules was visually confirmed by the fact that the hydrogel became more turbid at high NaCl concentration (Figure 8e and f). Notably, the fracture strain of these gels remained essentially constant (Figure 8c). These results demonstrate that the mechanical properties of the OEG/PAAm DN hydrogels could also be controlled by varying the salt concentration.

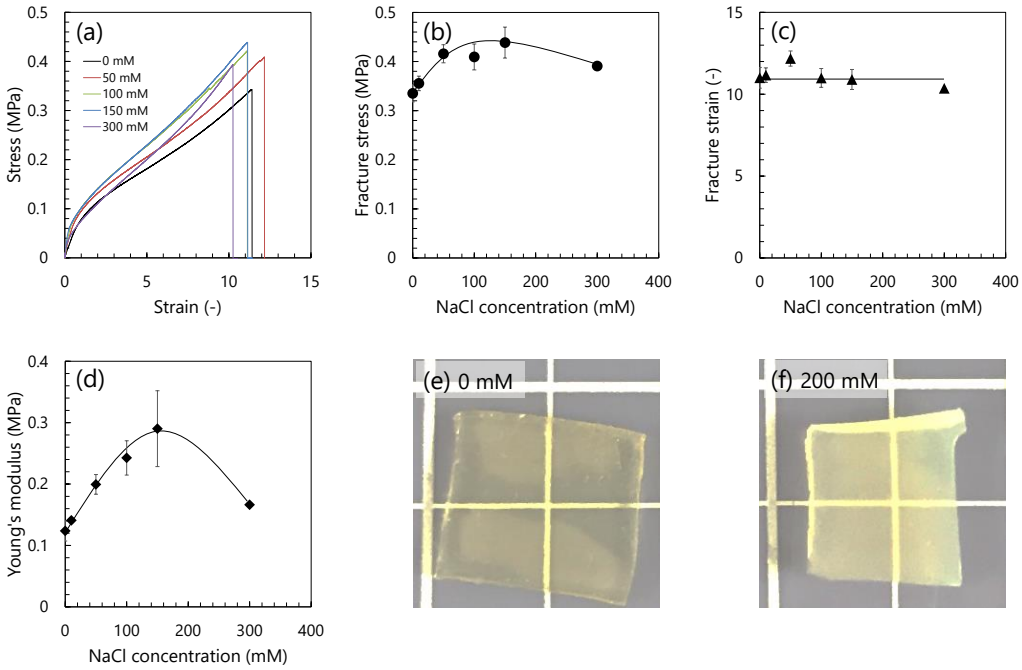

Figure 8. Effect of NaCl concentration on the mechanical behavior of OEG/PAAm DN hydrogels. (a) Stress–strain curves of OEG/PAAm DN hydrogels prepared with different NaCl concentrations. NaCl concentration dependency of (b) fracture stress, (c) fracture strain, and (d) Young's modulus. (e, f) Photographs of the OEG/PAAm DN hydrogel prepared using (e) 0 and (f) 200 mM of NaCl aqueous solution. The OEG and MBAA concentrations in OEG/PAAm DN hydrogels are 5 wt.% and 0.1% of AAm in moles, respectively.

Universality of the self-healing and strain rate-independent mechanical behavior based on thixotropic sacrificial network

Above results demonstrate that the thixotropic sacrificial network is key factor to show both strain rate-independent deformation and self-healing property of DN gels. we demonstrate the universality of the concept using another thixotropic sacrificial network.

We adopt a silica nanoparticle-based sacrificial network in ionic liquid medium. The silica nanoparticle-based gel network formed in ionic liquid show the frequency independent G' and thixotropic property.[44-46] Kamio *et al.* developed DN gels using the silica nanoparticle-based sacrificial network.[32, 34] This DN gels should also show strain softening, large mechanical hysteresis, and self-healing property. To confirm this assumption, we measured stress–strain curves of the silica nanoparticle-based DN gels with various strain rates. As shown in Figure S5, the change in stress–strain curves of the silica nanoparticle-based DN gels was very small over a wide strain rate range of 0.05–0.48 s^{-1}. This indicates that the strain rate-independent and self-healing property based on the thixotropic sacrificial network is the universal phenomenon regardless of gel network and solvent.

CONCLUSIONS

The one-pot synthesis method employed in this study enabled the facile synthesis of DN hydrogels in various shapes. The thixotropic OEG network in the OEG/PAAm DN hydrogels acted as an efficient energy dissipator and imparted a strain rate-independent self-healing mechanical behavior to the DN hydrogels. The quasi-elastic behavior of the thixotropic OEG hydrogels could be attributed to the rigidity of the OEG molecules that form fibrous networks via dynamic non-covalent intermolecular interactions. The mechanical properties of the OEG/PAAm DN hydrogels could be easily tuned by the concentration of PAAm network crosslinker or salt, which influences the structure of OEG network. We confirmed the universality of our concept because the strain rate-independent and self-healing mechanical behavior is observed not only in the OEG/PAAm DN hydrogels but also in the silica nanoparticle-based DN gels. This study presents a straightforward route to prepare novel DN hydrogels composed of supramolecular structures as

energy dissipators. The strain rate-independent and self-recovering mechanical behavior of these novel hydrogels is expected to broaden their potential functional applications.

ASSOCIATED CONTENT

Supporting Information.

The following files are available free of charge. Digital photograph of the precursor of OEG/PAAm DN hydrogel (OEG gel with AAm monomer), polarized microscopy image of OEG/PAAm DN hydrogel under crossed nicols configuration, cyclic loading–unloading curves of PAAm SN hydrogel, DSC curves of OEG/PAAm hydrogel, stress–strain curves of silica nanoparticle-based DN gels obtained at different strain rate, OEG synthesis reaction scheme. (PDF) A movie of OEG gel with AAm monomer under vortex mixing. (MP4)

AUTHOR INFORMATION

Corresponding Author

Jian Ping Gong − Faculty of Advanced Life Science, Hokkaido University, N21W11, Kita-ku, Sapporo, Hokkaido 001-0021, Japan and Institute for Chemical Reaction Design and Discovery (WPI-ICReDD), Hokkaido University, N21W10, Kita-ku, Sapporo, Hokkaido 001-0021, Japan (https://orcid.org/0000-0003-2228-2750; E-mail: gong@sci.hokudai.ac.jp).

Notes

The authors declare no competing financial interest.

ACKNOWLEDGMENT

This research was supported by JSPS KAKENHI grant numbers 19J11528 and 17H06144. The World Premier International Research Initiative (WPI), MEXT, Japan, established the Institute for Chemical Reaction Design and Discovery (WPI-ICReDD). The authors thank Ms. Miyuki Matsumoto (Hokkaido University) for her support in the experiments.

REFERENCES

(1) Nguyen, K. T.; West, J. L. Photopolymerizable hydrogels for tissue engineering applications. *Biomaterials* **2002**, *23*, 4307-4314.

(2) Lee, K. Y.; Mooney, D. J. Hydrogels for Tissue Engineering. *Chem. Rev.* **2001**, *101* (7), 1869-1880.

(3) Qiu, Y.; Park, K. Environment-sensitive hydrogels for drug delivery. *Adv. Drug Deliv. Rev.* **2001**, *53*, 321-339.

(4) Hoare, T. R.; Kohane, D. S. Hydrogels in drug delivery: Progress and challenges. *Polymer* **2008**, *49* (8), 1993-2007.

(5) Hoffman, A. S. Hydrogels for biomedical applications. *Adv. Drug Deliv. Rev.* **2012**, *64*, 18-23.

(6) Richter, A.; Paschew, G.; Klatt, S.; Lienig, J.; Arndt, K.-F.; Adler, H.-J. P. Review on Hydrogel-based pH Sensors and Microsensors. *Sensors* **2008**, *8*, 561-581.

(7) Kamoun, E. A.; Kenawy, E. S.; Chen, X. A review on polymeric hydrogel membranes for wound dressing applications: PVA-based hydrogel dressings. *J. Adv. Res.* **2017**, *8* (3), 217-233.

(8) Sakai, T.; Matsunaga, T.; Suzuki, S.; Sasaki, N.; Yamamoto, Y.; Shibayama, M.; Ito, C.; Yoshida, R.; Chung, U.-i. Design and Fabrication of a High-Strength Hydrogel with Ideally Homogeneous Network Structure from Tetrahedron-like Macromonomers. *Macromolecules* **2008**, *41*, 5379-5384.

(9) Okumura, Y.; Ito, K. The Polyrotaxane Gel: A Topological Gel by Figure-of-Eight Cross-links. *Adv. Mater.* **2001**, *13* (7), 485-487.

(10) Haraguchi, K.; Takehisa, T. Nanocomposite Hydrogels: A Unique Organic–Inorganic Network Structure with Extraordinary Mechanical, Optical, and Swelling/De-swelling Properties. *Adv. Mater.* **2002**, *14* (16), 1120-1124.

(11) Gong, J. P.; Katsuyama, Y.; Kurokawa, T.; Osada, Y. Double-Network Hydrogels with Extremely High Mechanical Strength. *Adv. Mater.* **2003**, *15* (14), 1155-1158.

(12) Liu, C.; Morimoto, N.; Jiang, L.; Kawahara, S.; Noritomi, T.; Yokoyama, H.; Mayumi, K.; Ito, K. Tough hydrogels with rapid self-reinforcement. *Science* **2021**, *372* (6546), 1078-1081.

(13) Yu, Q. M.; Tanaka, Y.; Furukawa, H.; Kurokawa, T.; Gong, J. P. Direct Observation of Damage Zone around Crack Tips in Double-Network Gels. *Macromolecules* **2009**, *42* (12), 3852-3855.

(14) Gong, J. P. Why are double network hydrogels so tough? *Soft Matter* **2010**, *6* (12), 2583–2590.

(15) Hu, J.; Hiwatashi, K.; Kurokawa, T.; Liang, S. M.; Wu, Z. L.; Gong, J. P. Microgel-Reinforced Hydrogel Films with High Mechanical Strength and Their Visible Mesoscale Fracture Structure. *Macromolecules* **2011**, *44* (19), 7775-7781.

(16) Nakajima, T.; Sato, H.; Zhao, Y.; Kawahara, S.; Kurokawa, T.; Sugahara, K.; Gong, J. P. A Universal Molecular Stent Method to Toughen any Hydrogels Based on Double Network Concept. *Adv. Funct. Mater.* **2012**, *22* (21), 4426-4432.

(17) Nakajima, T.; Fukuda, Y.; Kurokawa, T.; Sakai, T.; Chung, U.-i.; Gong, J. P. Synthesis and Fracture Process Analysis of Double Network Hydrogels with a Well-Defined First Network. *ACS Macro Lett.* **2013**, *2* (6), 518-521.

(18) Nakajima, T.; Ozaki, Y.; Namba, R.; Ota, K.; Maida, Y.; Matsuda, T.; Kurokawa, T.; Gong, J. P. Tough Double-Network Gels and Elastomers from the Nonprestretched First Network. *ACS Macro Lett.* **2019**, *8* (11), 1407-1412.

(19) Lin, W.-C.; Fan, W.; Marcellan, A.; Hourdet, D.; Creton, C. Large Strain and Fracture Properties of Poly(dimethylacrylamide)/Silica Hybrid Hydrogels. *Macromolecules* **2010**, *43* (5), 2554-2563.

(20) Henderson, K. J.; Zhou, T. C.; Otim, K. J.; Shull, K. R. Ionically Cross-Linked Triblock Copolymer Hydrogels with High Strength. *Macromolecules* **2010**, *43* (14), 6193-6201.

(21) Haque, M. A.; Kurokawa, T.; Kamita, G.; Gong, J. P. Lamellar Bilayers as Reversible Sacrificial Bonds To Toughen Hydrogel: Hysteresis, Self-Recovery, Fatigue Resistance, and Crack Blunting. *Macromolecules* **2011**, *44* (22), 8916-8924.

(22) Sun, J. Y.; Zhao, X.; Illeperuma, W. R.; Chaudhuri, O.; Oh, K. H.; Mooney, D. J.; Vlassak, J. J.; Suo, Z. Highly stretchable and tough hydrogels. *Nature* **2012**, *489* (7414), 133-136.

(23) Chen, Q.; Zhu, L.; Zhao, C.; Wang, Q.; Zheng, J. A robust, one-pot synthesis of highly mechanical and recoverable double network hydrogels using thermoreversible sol-gel polysaccharide. *Adv. Mater.* **2013**, *25* (30), 4171-4176.

(24) Sun, T. L.; Kurokawa, T.; Kuroda, S.; Ihsan, A. B.; Akasaki, T.; Sato, K.; Haque, M. A.; Nakajima, T.; Gong, J. P. Physical hydrogels composed of polyampholytes demonstrate high toughness and viscoelasticity. *Nat. Mater.* **2013**, *12* (10), 932-937.

(25) Mayumi, K.; Marcellan, A.; Ducouret, G.; Creton, C.; Narita, T. Stress–Strain Relationship of Highly Stretchable Dual Cross-Link Gels: Separability of Strain and Time Effect. *ACS Macro Lett.* **2013**, *2* (12), 1065-1068.

(26) Kean, Z. S.; Hawk, J. L.; Lin, S.; Zhao, X.; Sijbesma, R. P.; Craig, S. L. Increasing the maximum achievable strain of a covalent polymer gel through the addition of mechanically invisible cross-links. *Adv. Mater.* **2014**, *26* (34), 6013-6018.

(27) Long, R.; Mayumi, K.; Creton, C.; Narita, T.; Hui, C.-Y. Time Dependent Behavior of a Dual Cross-Link Self-Healing Gel: Theory and Experiments. *Macromolecules* **2014**, *47* (20), 7243-7250.

(28) Hu, X.; Vatankhah-Varnoosfaderani, M.; Zhou, J.; Li, Q.; Sheiko, S. S. Weak Hydrogen Bonding Enables Hard, Strong, Tough, and Elastic Hydrogels. *Adv. Mater.* **2015**, *27* (43), 6899-6905.

(29) Neal, J. A.; Mozhdehi, D.; Guan, Z. Enhancing mechanical performance of a covalent self-healing material by sacrificial noncovalent bonds. *J. Am. Chem. Soc.* **2015**, *137* (14), 4846-4850.

(30) Zheng, S. Y.; Ding, H.; Qian, J.; Yin, J.; Wu, Z. L.; Song, Y.; Zheng, Q. Metal-Coordination Complexes Mediated Physical Hydrogels with High Toughness, Stick–Slip Tearing Behavior, and Good Processability. *Macromolecules* **2016**, *49* (24), 9637-9646.

(31) Tang, Z.; Huang, J.; Guo, B.; Zhang, L.; Liu, F. Bioinspired Engineering of Sacrificial Metal–Ligand Bonds into Elastomers with Supramechanical Performance and Adaptive Recovery. *Macromolecules* **2016**, *49* (5), 1781-1789.

(32) Kamio, E.; Yasui, T.; Iida, Y.; Gong, J. P.; Matsuyama, H. Inorganic/Organic Double-Network Gels Containing Ionic Liquids. *Adv. Mater.* **2017**, *29* (47), 1704118.

(33) Mihajlovic, M.; Staropoli, M.; Appavou, M. S.; Wyss, H. M.; Pyckhout-Hintzen, W.; Sijbesma, R. P. Tough Supramolecular Hydrogel Based on Strong Hydrophobic Interactions in a Multiblock Segmented Copolymer. *Macromolecules* **2017**, *50* (8), 3333-3346.

(34) Yasui, T.; Kamio, E.; Matsuyama, H. Inorganic/Organic Double-Network Ion Gels with Partially Developed Silica-Particle Network. *Langmuir* **2018**, *34* (36), 10622-10633.

(35) Teng, L.; Chen, Y.; Jin, M.; Jia, Y.; Wang, Y.; Ren, L. Weak Hydrogen Bonds Lead to Self-Healable and Bioadhesive Hybrid Polymeric Hydrogels with Mineralization-Active Functions. *Biomacromolecules* **2018**, *19* (6), 1939-1949.

(36) Yoshida, M.; Koumura, N.; Misawa, Y.; Tamaoki, N.; Matsumoto, H.; Kawanami, H.; Kazaoui, S.; Minami, N. Oligomeric Electrolyte as a Multifunctional Gelator. *J. Am. Chem. Soc.* **2007**, *129*, 11039-11041.

(37) Misawa, Y.; Koumura, N.; Matsumoto, H.; Tamaoki, N.; Yoshida, M. Hydrogels Based on Surfactant-Free Ionene Polymers with N,N′-(p-Phenylene)dibenzamide Linkages. *Macromolecules* **2008**, *41*, 8841-8846.

(38) Kundu, S. K.; Osaka, N.; Matsunaga, T.; Yoshida, M.; Shibayama, M. Structural Characterization of Ionic Gelator Studied by Dynamic Light Scattering and Small-Angle Neutron Scattering. *J. Phys. Chem. B* **2008**, *112*, 16469-16477.

(39) Kundu, S. K.; Matsunaga, T.; Yoshida, M.; Shibayama, M. Rheological Study on Rapid Recovery of Hydrogel Based on Oligomeric Electrolyte. *J. Phys. Chem. B* **2008**, *112*, 11537-11541.

(40) Kundu, S. K.; Yoshida, M.; Shibayama, M. Effect of Salt Content on the Rheological Properties of Hydrogel Based on Oligomeric Electrolyte. *J. Phys. Chem. B* **2010**, *114*, 1541-1547.

(41) Yoshida, M. Ionic gelators: oligomeric and polymeric electrolytes as novel gel forming materials. *Chem. Rec.* **2010**, *10* (4), 230-242.

(42) Webber, R. E.; Creton, C.; Brown, H. R.; Gong, J. P. Large Strain Hysteresis and Mullins Effect of Tough Double-Network Hydrogels. *Macromolecules* **2007**, *40* (8), 2919-2927.

(43) Nakajima, T.; Furukawa, H.; Tanaka, Y.; Kurokawa, T.; Osada, Y.; Gong, J. P. True Chemical Structure of Double Network Hydrogels. *Macromolecules* **2009**, *42* (6), 2184-2189.

(44) Ueno, K.; Hata, K.; Katakabe, T.; Kondoh, M.; Watanabe, M. Nanocomposite ion gels based on silica nanoparticles and an ionic liquid: ionic transport, viscoelastic properties, and microstructure. *J. Phys. Chem. B* **2008**, *112* (30), 9013-9019.

(45) Ueno, K.; Imaizumi, S.; Hata, K.; Watanabe, M. Colloidal interaction in ionic liquids: effects of ionic structures and surface chemistry on rheology of silica colloidal dispersions. *Langmuir* **2009**, *25* (2), 825-831.

(46) Ueno, K.; Watanabe, M. From colloidal stability in ionic liquids to advanced soft materials using unique media. *Langmuir* **2011**, *27* (15), 9105-9115.